

Nodal Quasiparticle Dispersion in Strongly Correlated d-wave Superconductors

Mohit Randeria,^{1,2} Arun Paramakanti,³ and Nandini Trivedi^{1,2}

¹*Department of Physics, University of Illinois at Urbana-Champaign, IL 61801*

²*Department of Theoretical Physics, Tata Institute of Fundamental Research, Mumbai 400 005, India*

³*Department of Physics and Kavli Institute for Theoretical Physics,
University of California, Santa Barbara, CA 93106-4030*

We analyze the effects of a \mathbf{k} -dependent self-energy on the photoemission momentum distribution curve (MDC) dispersion and lineshape. We illustrate this general analysis by a detailed examination of nodal quasiparticles in high Tc cuprates. Using variational results for the nodal quasiparticle Z , which varies rapidly with hole doping x , and v_F^{low} , which is independent of x , we show that the high energy dispersion $v_F^{\text{high}} = v_F^{\text{low}}/Z$, so that it is much larger than the bare band structure dispersion and also exhibits strong doping dependence in good agreement with recent photoemission data.

Nodal quasiparticles (QP's) are the dominant low-lying excitations in the superconducting state of the high Tc superconductors, and have been the focus of intense experimental and theoretical investigation [1]. In particular, angle resolved photoemission spectroscopy (ARPES), exploiting the simple Lorentzian lineshape of momentum distribution curves (MDC's) [2], has provided a great deal of insight into the nodal QP weight and dispersion [2, 3, 4, 5, 6, 7, 8]. Two important questions are: (i) What constraints do these experiments place on a model for the superconducting state? (ii) To what extent are nodal QP properties determined purely by strong electronic interactions?

The purpose of this Letter is twofold. First, we examine the effect of the \mathbf{k} -dependence of the electronic self energy on the analysis of MDC's for gapless nodal QP's. Specifically, we determine how this affects the MDC dispersion, after clarifying the constraints under which the MDC lineshape is Lorentzian. This is important, because the usual basis for understanding a Lorentzian lineshape is a \mathbf{k} -independent self-energy [9], which is certainly sufficient but by no means necessary as shown here.

The second goal is to use the above formalism to gain insight into some unusual aspects of the nodal QP dispersion in the high Tc superconductors. Some time ago we predicted, on the basis of a variational calculation[10] for a Hubbard model that the nodal QP spectral weight Z vanishes linearly with hole doping x even though their Fermi velocity v_F^{low} remains doping independent as $x \rightarrow 0$. (We use the notation v_F^{low} here, rather than the more conventional v_F , to clearly distinguish it from v_F^{high} defined below). These predictions have now been verified in some detail by angle-resolved photoemission spectroscopy (ARPES) experiments [6, 7, 8].

These same experiments also show an unusual doping dependence of the *high energy dispersion*, at binding energies larger than the much-studied kink [5, 6, 7, 11, 12] in the nodal MDC dispersion. The “high energy” Fermi velocity v_F^{high} , at energies of around 150 to 200 meV, is experimentally found [5, 6, 7] to be quite strongly doping dependent and *increases* markedly with underdoping, where as one might have naively expected the “bands”

to become narrower with decreasing x . This behavior of v_F^{high} is also in marked contrast with both the Fermi velocity at E_F which, as stated above, is x -independent, and the “bare” band-structure Fermi velocity v_F^0 which has a rather weak x -dependence.

In this Letter, we show that this surprising behavior of $v_F^{\text{high}}(x)$ follows directly from the same theory [10] which predicted $Z(x)$ and the x -independent v_F^{low} . As discussed below, the results for $Z(x)$ and v_F^{low} imply strong constraints on *both* the ω - and \mathbf{k} -dependence of the real part of the self energy $\Sigma'(\mathbf{k}, \omega)$. Specifically, both $\partial\Sigma'/\partial\omega$ and $\partial\Sigma'/\partial k$ must exhibit $1/x$ singularities. The strong \mathbf{k} -dependence is somewhat unexpected, and we show here that it has an important effect on the “high energy” dispersion:

$$v_F^{\text{high}} = v_F^0 + \partial\Sigma'/\partial k = v_F^{\text{low}}/Z \quad (1)$$

leading to a strong doping dependence in v_F^{high} , including an $1/x$ divergence as the hole doping $x \rightarrow 0$. We make detailed quantitative comparison of our results with existing ARPES data, and conclude with comments on the kink in the MDC dispersion.

MDC analysis: We first develop the formalism for the analysis of photoemission MDC's, focusing on two points *not* emphasized in the literature: the conditions under which the MDC lineshape can be Lorentzian despite \mathbf{k} -dependence of the self energy, and the role of $\partial\Sigma'/\partial k$ in the MDC dispersion. Recall that the ARPES intensity from a two-dimensional system is given by [13] $I(\mathbf{k}, \omega) = I_0(\mathbf{k})f(\omega)A_{\mathbf{k}, \omega}$ where I_0 contains the dipole matrix element and kinematical factors, $f(\omega)$ is the Fermi function and $A_{\mathbf{k}, \omega}$ is the one-particle spectral function. Here \mathbf{k} is the 2D momentum and ω the energy measured from the chemical potential. The usual energy distribution curve (EDC) method views ARPES data as a function of energy at fixed \mathbf{k} . The MDC method, on the other hand, analyzes $I(\mathbf{k}, \omega)$ as a function of \mathbf{k} , along a suitable chosen cut in \mathbf{k} -space, for fixed ω . The MDC method is more powerful than the traditional EDC for studying gapless excitations, because of the simple Lorentzian

MDC lineshape and also the ease of unambiguously identifying the extrinsic background.

Here we are specifically interested in the MDC's for a $d_{x^2-y^2}$ superconductor for k along the zone diagonal, so that the “off-diagonal” self energy (gap function) vanishes. The formalism derived is obviously applicable near the Fermi surface of any normal metal also. The spectral function is then given by:

$$A_{\mathbf{k},\omega} = \frac{1}{\pi} \frac{|\Sigma''(\mathbf{k},\omega)|}{[\omega - \epsilon_0(\mathbf{k}) + \mu_0 - \Sigma'(\mathbf{k},\omega)]^2 + [\Sigma''(\mathbf{k},\omega)]^2} \quad (2)$$

where $\epsilon_0(\mathbf{k})$ and μ_0 are the “bare” dispersion and chemical potential, and $\Sigma = \Sigma' + i\Sigma''$ the self-energy.

The “renormalized” k_F is defined by the condition $\epsilon_0(\mathbf{k}_F) - \mu_0 + \Sigma'(\mathbf{k}_F, 0) = 0$. In case interactions lead to no change in the k_F , this places a constraint $\Sigma'(\mathbf{k}_F, 0) = 0$ on the real part of the self energy. We now expand in small $|k - k_F| \ll k_F$ in the vicinity of the node at k_F , keeping ω arbitrary for the moment. Linearizing the dispersion, we thus get

$$\epsilon_0(\mathbf{k}) - \mu_0 + \Sigma'(\mathbf{k}_F, 0) \simeq v_F^0(k - k_F) \quad (3)$$

where v_F^0 is called the bare Fermi velocity.

We next assume $\Sigma''(\mathbf{k},\omega) \simeq \Sigma''(\mathbf{k}_F,\omega)$ which is equivalent to setting the first correction

$$\partial\Sigma''(\mathbf{k}_F,\omega)/\partial k = 0, \quad (4)$$

for all ω of interest. This is a *necessary* condition for a Lorentzian lineshape in $(k - k_F)$, since without it the numerator in eq. (2) would have a term linear in $(k - k_F)$ which would make the expression non-Lorentzian. The Kramers-Krönig transformation of the above condition implies that $\partial\Sigma'/\partial k$ can only be a constant independent of ω , a condition we will need to use below. (In the experiments, an additional constraint for a Lorentzian MDC is that the matrix element prefactor I_0 should be \mathbf{k} -independent in the range of relevant \mathbf{k} 's.)

With this one assumption, the spectral function $A_{\mathbf{k},\omega}$ is easily shown to be a Lorentzian in $(k - k_F)$ peaked at

$$k(\omega) = k_F + \frac{\omega - [\Sigma'(\mathbf{k}_F,\omega) - \Sigma'(\mathbf{k}_F,0)]}{(v_F^0 + \partial\Sigma'/\partial k)} \quad (5)$$

with a width $\Delta k = |\Sigma''(\mathbf{k}_F,\omega)|/(v_F^0 + \partial\Sigma'/\partial k)$. The dispersion of this Lorentzian MDC is then obtained from

$$\frac{dk}{d\omega} = \frac{1 - \partial\Sigma'(\mathbf{k}_F,\omega)/\partial\omega}{v_F^0 + \partial\Sigma'/\partial k} \equiv \frac{\zeta(\omega)}{v_F^0 + \partial\Sigma'/\partial k}, \quad (6)$$

where the denominator is ω -independent and evaluated at $\mathbf{k}=\mathbf{k}_F$, but the numerator at arbitrary ω and $\mathbf{k}=\mathbf{k}_F$.

In the limit $\omega \rightarrow 0$, the MDC dispersion of eq. (6) yields the standard result. Defining the low-energy renormalized Fermi velocity v_F^{low} via $1/v_F^{\text{low}} = dk/d\omega(\omega \rightarrow 0)$, we get

$$v_F^{\text{low}} = Z [v_F^0 + \partial\Sigma'/\partial k]. \quad (7)$$

Here the QP weight Z is defined by

$$Z \equiv 1/\zeta(\omega \rightarrow 0) = 1/[1 - \partial\Sigma'/\partial\omega], \quad (8)$$

with $\partial\Sigma'/\partial\omega$ is evaluated at $(\mathbf{k} = \mathbf{k}_F, \omega = 0)$.

On the other hand, one can quite generally show [14] that at intermediate to high energies, $|\partial\Sigma'/\partial\omega| \ll 1$, so that $\zeta(\omega) \approx 1$. Then the corresponding high energy $1/v_F^{\text{high}} = dk/d\omega$ is given by

$$v_F^{\text{high}} \approx v_F^0 + \partial\Sigma'/\partial k, \quad (9)$$

which together with eq. (7) leads to the result eq. (1) stated in the Introduction. Here $\partial\Sigma'/\partial k$ is an ω -independent constant as discussed in connection with the necessary conditions (Kramers-Krönig transform of eq. (4)) for Lorentzian lineshapes.

The above results are completely general, and we next illustrate this formalism for the low and high energy dispersion of nodal QPs in the cuprates.

Low energy properties $Z(x)$ and $v_F^{\text{low}}(x)$: In Ref. [10] we have presented a $T = 0$ variational theory, building on early ideas of Anderson [15], for the strongly correlated d-wave SC and its low-lying excitations, examining how they evolve as a function of hole doping x from a Fermi liquid state at overdoping $x \gtrsim 0.35$ to a Mott insulator at half-filling ($x = 0$). Here we summarize specific results from Ref. [10] which relate to doping dependence of the nodal QP spectral weight $Z(x)$ and Fermi velocity $v_F^{\text{low}}(x)$, and describe their implications for $\Sigma'(\mathbf{k},\omega)$.

We begin by emphasizing that these results for the nodal QP were *not* obtained by working with a variational excited state, e.g., a Gutzwiller projected Bogoliubov QP. Given the very broad linewidth of the spectral function, it is difficult to use simple variational excited states to obtain useful results on the coherent QP piece; see Ref. [16]. Instead we focused on the *singularities* as a function of \mathbf{k} in the energy-integrated moments of the spectral function to extract information related to gapless QPs. In particular, Z was extracted from the jump in $\int_{-\infty}^0 d\omega A_{\mathbf{k},\omega} = n(\mathbf{k})$ and v_F^{low} from the slope discontinuity of $\int_{-\infty}^0 d\omega \omega A_{\mathbf{k},\omega}$ at $\mathbf{k} = \mathbf{k}_F$ [16].

We found that [10] $Z(x)$ decreases with underdoping, with $Z \sim x$ [17] as $x \rightarrow 0$, and remarkably that $v_F^{\text{low}}(x)$ is essentially doping independent and remains finite as $x \rightarrow 0$. Using eq. (8) one must then conclude from the calculated $Z(x)$ that $|\partial\Sigma'/\partial\omega| \sim 1/x$ as $x \rightarrow 0$. Further, using eq. (7), the calculated $v_F^{\text{low}}(x)$ implies a compensating divergence $\partial\Sigma'/\partial k \sim Ja/x$, where the superexchange J and lattice constant a enter on dimensional grounds.

In the $x \rightarrow 0$ limit one thus obtains $Z \sim x$, with a renormalized low energy Fermi velocity $v_F^{\text{low}}(x \rightarrow 0) = CJa$, where C is a dimensionless constant of order unity. Remarkably these results are *independent* of the bare band-structure dispersion and thus “universal”. From our numerical results [10] we find $C \approx 4.5$. We emphasize

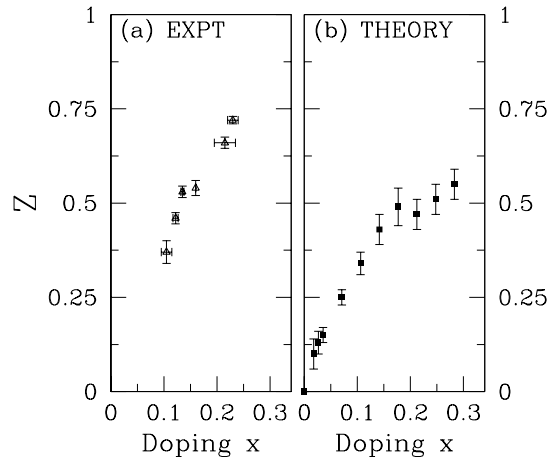


FIG. 1: **(a)** Doping dependence of the nodal QP weight Z in Bi2212 extracted from data in Ref.[6] using $Z = 1/(1 + \lambda)$. The doping x was calculated from their sample T_c using the empirical formula [18]: $86(x - 0.16)^2 = (1 - T_c/T_c^{\max})$, with $T_c^{\max} = 91K$ for their samples. **(b)** $Z(x)$ predicted from a variational approach shows that $Z \rightarrow 0$ on underdoping, and is in good agreement with the experimental trend and values.

that these non-trivial results for the doping variation of Z and v_F^{low} are non-perturbative, strong coupling results which come from a variational calculation which properly takes into account the strong local Coulomb repulsion.

High Energy Dispersion $v_F^{\text{high}}(x)$: Combining all the results described above, we see from $v_F^{\text{high}} = v_F^{\text{low}}/Z(x)$, that we expect $v_F^{\text{high}} \gg v_F^{\text{low}}$ and also that it will show considerable doping dependence and increase with underdoping, given the predicted $Z(x)$. Moreover, using eq. (9) and the form of $\partial\Sigma'/\partial k$ derived above, it immediately follows that there is Ja/x divergence in v_F^{high} , which at small enough x is much larger than and independent of the “bare” band-structure v_F^0 .

Comparison with ARPES Experiments: We are now in a position to compare the theoretical results derived above with existing ARPES data. In Fig. 1 we plot the nodal QP weight Z as a function of hole doping x . Fig. 1(a) shows Z extracted from the experimental data of Ref. [6] on Bi2212. These authors plot $\lambda = -\partial\Sigma'/\partial\omega$ as a function of doping, from which we obtain Z using $Z = 1/(1 + \lambda)$. In Fig. 1(b) we plot the nodal $Z(x)$ obtained from our variational calculation [10] and find very good agreement [19] between theory and experiment. We should note that to leading order in J/t [17] the calculated $Z(x)$ is independent of the choice of input parameters in our theory [20]. The nodal $Z(x)$ has also been reported for LSCO [8], but in arbitrary units, which makes a quantitative comparison difficult, however the trend is qualitatively similar to our theoretical prediction.

We next show in Fig. 2 the low energy Fermi velocity v_F^{low} for nodal QPs in units of $\text{eV}\cdot\text{\AA}$ as a function of dop-

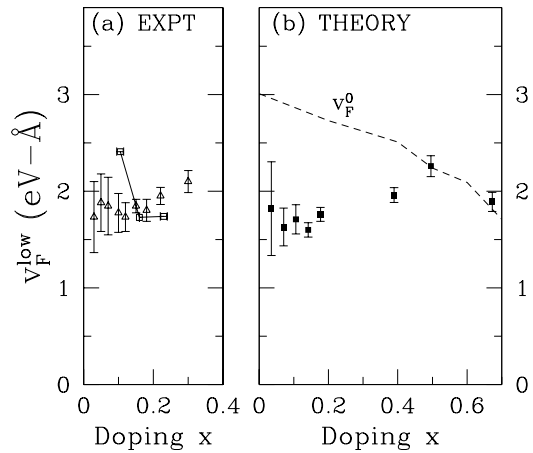


FIG. 2: **(a)** The Fermi velocity v_F^{low} in Bi2212 (open squares joined by a line as guide to the eye, Ref.[6]) and LSCO (open triangles, Ref.[7]) is nearly doping independent with a similar value in various cuprates (see Ref.[7] for additional data). **(b)** Theoretically predicted v_F^{low} using a variational approach is constant for $x \lesssim 0.2$, independent of the bare band structure (“universal”), and crosses over to the bare Fermi velocity (v_F^0 , dashed line) at large x . The values and trend are in good agreement with experiment [7].

ing. The experimental results shown in Fig. 2(a) are obtained from the MDC dispersion at E_F for LSCO (open triangles from Ref. [7]) and for Bi2212 (open squares from Ref. [6]). In Fig. 2(b) we show the “bare” v_F^0 (dashed line), which has a weak doping dependence coming from the change of the chemical potential in the bare tight-binding model [20]. The renormalized low energy Fermi velocity v_F^{low} is however found to be smaller and nearly doping independent, within the error bars of the theoretical calculation [19], for the hole doping range $x \leq 0.2$, its scale being set by Ja as explained in detail above.

Finally we come to the comparison of theory and experiment for the high energy dispersion v_F^{high} in Fig. 3. The data in Fig. 3(a) are obtained from the high energy MDC dispersion for LSCO (open squares from Ref. [7]) and for Bi2212 (open triangles from Ref. [6]). In Fig. 3(b) we plot the theoretical estimate of the high energy velocity using the expression derived above $v_F^{\text{high}} = v_F^{\text{low}}/Z(x)$. We find good agreement with the data over the range of dopings from $x \gtrsim 0.05$ both in terms of magnitude and overall trend. There is a $1/x$ divergence in the theoretical value at small x , for reasons explained above, but evidence for that in the very low doping data in LSCO is not clear. Quite independent of our variational calculation, the general result $v_F^{\text{high}} = v_F^{\text{low}}/Z(x)$ derived above, together with the experimentally observed behavior of v_F^{low} (constant [7]) and of $Z(x)$ (vanishing as $x \rightarrow 0$ [8]) in LSCO, implies a v_F^{high} that increases strongly as $x \rightarrow 0$. We hope future experiments will clarify this situation.

Implications for the kink: The success of the theory

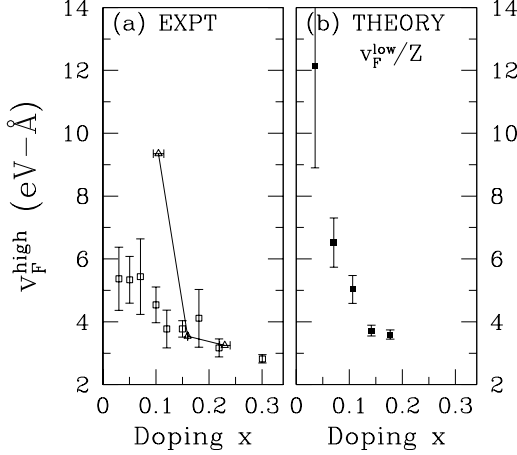


FIG. 3: **(a)** Doping dependence of the high energy energy velocity v_F^{high} above the kink in the MDC dispersion from data on Bi2212 (open squares joined by a line as guide to the eye, Ref.[6]) and LSCO (open triangles, Ref.[7]). **(b)** A variational calculation [19] of $v_F^{\text{high}} = v_F^{\text{low}}/Z$ shows that it increases on underdoping in agreement with the experimental trend and values for $x \gtrsim 0.05$.

described above leads to the obvious question: What is the origin and energy scale of the kink? By the "kink" we mean the sharp change in the observed MDC dispersion separating the low and high energy regimes which occurs at an energy scale of about 70 meV [5, 6, 7]. Its origin is controversial at present, with electrons interacting with either an optical phonon [5] or with the neutron resonance mode [11, 12] being the two likely scenarios.

We have presented here a framework for understanding the low and high energy limits MDC dispersion of eq. (6), in limits where the factor of $\zeta(\omega)$ goes to Z and unity respectively. This general framework cannot directly address precisely how and at what energy scale there is a transition from one limiting behavior to the other. The variational approach only permitted a calculation of the low energy behavior of the nodal QPs — its implications for v_F^{high} hinged upon the remarkable relationship between this high energy quantity and the low energy v_F^{low} and Z , which could be calculated. However, we emphasize that the variational calculation, which focuses on the strong Coulomb interactions, is able to give qualitative and semi-quantitative insights into the doping dependence of both the low and high energy dispersion of the nodal QPs. Thus it would be very surprising if the intermediate energy scale kink were not also dominated by strong electron-electron interaction effects.

Conclusions: To summarize, we first obtained the conditions, eq. (4) and its Kramers-Krönig transform, for a Lorentzian MDC lineshape, and then used this to derive the MDC dispersion eq. (6) and the linewidth, both of which involve the \mathbf{k} -dependence of the self energy in an essential way. We next showed how the high energy dis-

persion was related directly via eq. (1) to the QP spectral weight Z and the low-energy Fermi velocity v_F^{low} . We then illustrated this general formalism by using variational results for the nodal QP in the cuprates, where we showed that the $Z(x)$ was strongly doping dependent and vanishing as $x \rightarrow 0$, v_F^{low} was essentially doping independent, and $v_F^{\text{high}} = v_F^{\text{low}}/Z(x)$. All of these results were shown to be in good agreement with ARPES data.

Acknowledgments: We thank J. C. Campuzano, J. Fink, A. Fujimori, P. D. Johnson, A. Kaminski, A. J. Leggett and Z. X. Shen for stimulating discussions. MR and NT acknowledge support through DOE grant DEFG02-91ER45439 and DARPA grant N0014-01-1-1062; AP was supported by NSF grants DMR-9985255 and PHY-07949, and the Sloan and Packard foundations.

-
- [1] See, e.g., J. Orenstein and A.J. Millis, Science **288**, 468 (2000) for a review of earlier work.
 - [2] T. Valla, et al., Science **285**, 2110 (1999).
 - [3] A. Kaminski, et al., Phys. Rev. Lett. **84**, 1788 (2000); Phys. Rev. Lett. **86**, 1070 (2001).
 - [4] P.V. Bogdanov, et al., Phys. Rev. Lett. **85**, (2000).
 - [5] A. Lanzara, et al., Nature **412**, 510 (2001).
 - [6] P. D. Johnson, et al., Phys. Rev. Lett. **87**, 177007 (2001).
 - [7] X. J. Zhou, et al., Nature **423**, 398 (2003), and accompanying data on the Nature website.
 - [8] T. Yoshida, et al., cond-mat/0206469.
 - [9] See, e.g., J. C. Campuzano, M. R. Norman and M. Randeria, cond-mat/0209476.
 - [10] A. Paramekanti, M. Randeria and N. Trivedi, Phys. Rev. Lett. **87**, 217002 (2001).
 - [11] M. Eschrig and M. Norman, Phys. Rev. Lett. **85**, 3261 (2000); Phys. Rev. B **67**, 144503 (2003).
 - [12] Ar. Abanov, et al., Phys. Rev. Lett. **89**, 177002 (2002).
 - [13] M. Randeria, et al., Phys. Rev. Lett. **74**, 4951 (1995).
 - [14] We have checked this over a wide range of ω using phenomenological forms for $\Sigma''(\mathbf{k}, \omega)$ and Kramers-Krönig analysis.
 - [15] P. W. Anderson, Science **235**, 1196 (1987).
 - [16] A. Paramekanti, M. Randeria and N. Trivedi, cond-mat/0305611.
 - [17] The Gutzwiller approximation permits analytical calculation of many observables studied in Ref. [10] and gives $Z = 2x/(1+x)$ with $\mathcal{O}(xJ/t)$ corrections (see: R. Sen Sarma, M. Randeria and N. Trivedi, unpublished).
 - [18] M. R. Presland, et al., Physica C **176**, 95 (1991).
 - [19] The error bars in the theoretical estimates for Z and v_F^{low} are mainly due to a combination of limited resolution on a finite lattice in the numerics and from fits to the computed spectral function moments; see Ref. [16] for details. The error in $v_F^{\text{high}} = v_F^{\text{low}}/Z$ is a combination of these errors and grows with underdoping since $Z \rightarrow 0$.
 - [20] The input to the variational calculation is minimal: the bare nearest and next-nearest neighbor hoppings are $t = 300\text{meV}$ and $t' = t/4$ respectively (motivated by electronic structure calculations) and the superexchange $J = 100\text{meV}$ (motivated by neutron and Raman scattering experiments). For details, see Ref. [16].